Articles in PresS. J Appl Physiol (April 5, 2012). doi:10.1152/japplphysiol.01383.2011

Early apoptosis in different models of cardiac hypertrophy induced by high renin-angiotensin system activity involves CaMKII

by

J Omar Velez Rueda, Julieta Palomeque, Alicia Mattiazzi

Centro de Investigaciones Cardiovasculares, CONICET-La Plata, Facultad de Medicina, UNLP, Argentina.

Short title: Apoptosis in heart via RAAS and CaMKII

Key words: Angiotensin II, CaMKII, ROS, Hypertrophy, Apoptosis

Corresponding author: Julieta Palomeque

Centro de Investigaciones Cardiovasculares

Facultad de Medicina

La Plata

Argentina

Phone/fax: (54-221) 483-4833

Email: julip@aetos.med.unlp.edu.ar

ABSTRACT

Objective- To establish whether **1.** Hyperactivity of renin-angiotensin-aldosterone system (RAAS) produces apoptosis in early stages of cardiac disease; **2.** Ca^{2+}-Calmodulin dependent protein kinase II (CaMKII) is involved in these apoptotic events.

Methods- Two models of hypertrophy were used at an early stage of cardiac disease: spontaneously hypertensive rats (SHR) and Isoproterenol treated rats (Iso-rats).

Results- At 4 months, SHR showed blood pressure, aldosterone serum levels,-used as RAAS activity index-, and left ventricular mass index (LVMI), -used as hypertrophy index-, above control values by 84.2±2.6 mmHg, 211.2±25.8%, and 8.6±1.1 mg/mm, respectively. There was also an increase in apoptotis (Bax/Bcl-2 ratio and TUNEL positive cells) associated with an enhancement of CaMKII activity with respect to aged matched controls (P-CaMKII, 98.7±14.1 above control). Similar results were observed in 4 months old Iso-rats. Cardiac function studied by echocardiography, remained unaltered in all groups. Enalapril (Ena) treatment significantly prevented hypertrophy, apoptosis and CaMKII activity. Moreover, intracellular Ca^{2+} (Ca^{2+}_i) handling in isolated myocytes was similar between SHR, Iso-rats and their aged matched controls. However, SHR and Iso-rats showed a significant increase in $\cdot O_2$- generation (lucigenin) and lipid peroxidation (TBARS). In transgenic mice with targeted cardiomyocyte expression of a CaMKII inhibitory peptide (AC3-I) or a scrambled control peptide (AC3-C), Iso treatment increased TBARS in both strains whereas it increased CaMKII activity and apoptosis only in AC3-C mice.

Conclusions- Endogenous increases in RAAS activity induce ROS and CaMKII-dependent apoptosis *in vivo.* CaMKII activation could not be associated with Ca^{2+}_i increments and was directly related to the increase in oxidative stress.

INTRODUCTION

Experimental evidence indicates that a critical factor in the transition from compensated to non-compensated cardiac hypertrophy is myocyte cell loss by apoptosis and necrosis (42). The circulating levels of Angiotensin II (AngII) are increased in heart failure and may constitute one of the major causes of cell death in this transition (27). Moreover, activation of the multifunctional Ca^{2+}-Calmodulin Protein Kinase II (CaMKII), -being its δ isoform largely predominant in mammalian myocardium (46)- is a typical finding in heart failure from different etiologies. Activation of this kinase also constitutes a main step in the signaling cascade that leads to apoptosis following several cardiac insults like reperfusion injury (39), ionomycin, high extracellular K^+ concentration, intracellular acidosis and oxidative stress (28, 32, 47). Furthermore, intracellular reactive oxygen species (ROS) levels increase dramatically in models of structural heart disease (18) particularly those initiated by AngII (35). In recent *in vitro* experiments, we described an apoptotic pathway which involves increases in ROS produced by AngII and activation of CaMKII (28). Exogenous AngII administration has also been linked to CaMKII and apoptosis *in vivo* (11). Whether these events can also be triggered by exacerbated endogenous AngII production and which is their impact, if any, on cardiac function, remains unclear.

It has been shown that spontaneously hypertensive rats (SHR), one of the most used models for hypertrophy and heart failure studies, have high activity of the renin-angiotensin-aldosterone system (RAAS) (45) and increased CaMKII expression (17). Hagemann *et al* described that CaMKIIδ, is overexpressed in hearts from adult SHR (17). Furthermore, normotensive rats treated with high

doses of isoproterenol (Iso), also show high activity of RAAS (16). However, a possible association between endogenous levels of AngII in different early stages models of exacerbated RAAS activity and CaMKII-induced apoptosis has not been previously studied. Moreover, the functional consequences of RAAS exacerbation in early stages of heart disease are an uncharted territory. Taking advantage of these models, the present experiments were undertaken to investigate the early repercussion of high RAAS activity on CaMKII activation, apoptosis and cardiac function.

METHODS

Animals and protocols

Animals used in this study were maintained in accordance with the Guide for the Care and Use of Laboratory Animals [NIH Publication No. 85–23, revised 1996].

Male SHR and normotensive aged matched control Wistar rats were used. At 3 months, a group of SHR was treated with 10 mg/kg/day enalapril, an inhibitor of the angiotensin converting enzyme (ACE), in the drinking water for one month.

Normotensive Wistar rats were treated at 3 months with two subcutaneous injections of Isoproterenol (Iso) 250 mg/kg, separated by a 24 h interval according to a previously described protocol (34), in order to induce cardiac damage (3, 4, 30). Iso solution was prepared with sterile distilled acid water, to prevent Iso oxidation, immediately before injection. Control rats were injected with the solution without the drug. The rats treated with Iso were further randomly assigned to receive enalapril (Iso-Ena rats), (at the doses and way mentioned for SHR) or no drug (Iso rats). An additional group of rats, receiving only enalapril (Ena rats) was used as control. All treatments were performed for one month.

Before and after the treatment the animals were weighed, the systolic blood pressure was measured by the tail-cuff method, and echocardiographic examination was performed. Rats were then sacrificed, the heart was weighed and the tibia length (TL) was measured. Hearts were assigned for biochemical studies, immunohistochemical staining, ROS production determinations, or myocyte isolation for contractile and Ca^{2+}_i measurements.

Additionally, transgenic mice with cardiomyocyte-delimited transgenic expression of either a CaMKII inhibitory peptide (AC3-I) or a scrambled control peptide (AC3-C) were used. Breeding mates of these mice were generously supplied by Dr. Mark Anderson (University of Iowa, USA) and reproduced and genotyped in our laboratory. The mice were treated as the Iso-rats, i.e. animals were sacrificed one month after injections and the hearts were used for measuring ROS, CaMKII activity and apoptosis.

Aldosterone Plasma Levels

Aldosterone plasma levels were used as an index of AngII plasma levels (21) and RAAS activity. Blood samples were centrifuged at 13.500 rpm for 15 min and the plasma was stored at -80ºC until analysis. The plasma aldosterone concentration was measured by standard radioimmunoassay method according to manufacturer instructions.

Echocardiographic Examination

Echocardiogram was performed in each rat under light anesthesia (35 mg/kg sodium pentobarbital IP). Cardiac geometry and function were evaluated by 2-dimensional M-mode echocardiography with a 7-MHz linear transducer. All measurements, including left ventricular (LV) wall thickness and diastolic dimensions, were performed according to the American Society of Echocardiography method (31). LV mass was calculated as previously described (24).

Myocyte Isolation

Rats were anaesthetised by intra-abdominal injection of sodium pentobarbital and myocytes were isolated by enzymatic digestion (29) and kept in a HEPES buffered solution at room temperature (20-22 °C), until used.

Ca^{2+}_i and Cell Shortening

Isolated myocytes were loaded with Fura-2/AM (10 μmol/L for 15 min). Ca^{2+}_i was measured with an epi-fluorescence system (Ion Optix, Milton, MA). Briefly, dye-loaded cells were placed in a chamber on the stage of an inverted microscope (Nikon.TE 2000-U) and continuously superfused with a HEPES buffered solution at a constant flow of 1 mL/min at room temperature (20-22 °C) Myocytes were stimulated via two-platinum electrodes on either side of the bath at 0.5 Hz. Fura-2 fluorescence was taken as an index of the Ca^{2+}_i. Resting cell length and cell shortening were measured by a video-based motion detector (Ion Optix). Fluorescence and cell shortening data were stored for off-line analysis (ION WIZARD fluorescence analysis software).

ROS Determinations

Superoxide Anion ($\cdot O_2^-$) Production

Cardiac tissue slices from the left ventricle (1-5 mm) were obtained and kept at 4°C until assayed as previously described. Cardiac slices were kept in the assay buffer during 30 min in a metabolic incubator before anion superoxide ($\cdot O_2$-) production was measured by the lucigenin (5 μmol/L)-enhanced chemiluminescence method, after 20 min of incubation with lucigenin as previously described (8). The lucigenin-containing assay buffer with tissue

slices minus background was recorded. $\cdot O_2-$ production was normalized to mg/dwt/min. The increases in $\cdot O_2-$ production were expressed as differences from control values

Lipid Peroxidation

Lipid peroxidation was determined by measuring the rate of production of thiobarbituric acid reactive substances (TBARS), expressed as nmol/mg protein. Heart homogenates were centrifuged at 2.000xg for 10 min. Supernatants (0.5 mL) were mixed with 1.5 mL trichloroacetic acid (30% w/v) and 0.5 mL water, followed by boiling for 15 min. After cooling, absorbance was determined spectrophotometrically at 535 nm, using a ε value of 1.56 x 105 $(mmol/L)^{-1}$ cm^{-1} (5).

Western Blot

Hearts were freeze-clamped and pulverized. Briefly, 0.1 g of tissue was homogenized in 4 volumes of lysis buffer (in mmol/L, 30 KH_2PO_4, 25 NaF, 300 sucrose, 0.1 EDTA plus proteases inhibitor cocktail). Protein was measured by the Bradford method using BSA as standard. Lysates (~90µg of total protein) were separated per gel line in 10% SDS polyacrilamide gel (26) and transferred to polyvinylidene difluoride membranes. Blots were probed overnight with the following antibodies: Bcl-2 (Santa Cruz), Bax (Santa Cruz), Caspase-3 (Chemicon), P-CaMKII 1:1000 (Abcam,), CaMKIIδ 1:1000 (Santa Cruz), Thr^{17}-phosphorylated (P-Thr^{17}) of phospholamban (PLN) 1:5000 (Badrilla, Leeds, UK), PLN 1:5000 (Badrilla, Leeds, UK). CaMKIIδ, PLN and GAPDH signals were used to normalize the signal intensity of the different proteins, as it is mentioned under Results. Immunoreactivity was visualized by a peroxidase-

based chemiluminescence detection kit (Amersham Biosciences) using a Chemidoc Imaging system. The signal intensity of the bands in the immunoblots was quantified by densitometry, using Image J software (NIH). Some proteins, i.e. Bcl-2, could appear as one or two bands. It has been suggested that more than one band may correspond to differentially phosphorylated forms or cleavage products (6, 23, 44).Due to this variation we quantify the intensity of the two bands together when they appear.

Apoptosis Assays

Apoptosis was determined by TUNEL assay (In Situ Cell Death Detection Kit, TMR red, Roche, Mannheim, Germany). The TUNEL positive cells were imaged under a fluorescence microscope (200x magnification) and counted in 10 random fields for each experimental situation. The results were expressed as percentage of TUNEL positive cells related to total number of cells. DAPI (1ug/mL, 4′, 6-Diamidino-2-phenylindole dihydrochloride, Sigma, St Lous, MO) was used for nuclear staining. Apoptotic cell death was also assessed by immunoblotting, as described above, as the increase in the ratio between the apoptotic signals Bax and the anti-apoptotic signal Bcl-2 and the enhancement in the amount of the 17-kDa cleavage product of Caspase-3, indicating Caspase-3 activation (28).

Exercise tolerance

Rats were pretested for their treadmill running willingness at constant velocity of 15 m/min without slope, until animals became exhausted or until they completed a 15 min period.

Statistics

All data are presented as mean ± SEM. Comparisons within groups were made by either paired or unpaired Student's t test, as appropriate. One-way ANOVA was used for multigroup comparisons. The Newman-Keuls test was used to examine statistical differences observed with ANOVA. A value of $p<0.05$ was taken to indicate statistical significance.

RESULTS

High RAAS activity induced cardiac hypertrophy and apoptosis in SHR is associated with CaMKII activation

Aldosterone plasma levels and blood pressure were significantly increased in 4 months old SHR with respect to age matched normotensive controls rats (Figure 1***A*** and ***B***). Moreover, Figures 1***C*** to ***E*** show that SHR developed hypertrophy as indicated by the increase in the heart weight/tibia length (HW/TL) ratio, the cross sectional area (CSA) of the myocytes and the left ventricular mass index (LVMI) evaluated by echocardiography (see also Table 1). Representative images of echocardiography and left ventricle specimens obtained from each experimental group are shown in the right panels of Figure 1 (***D*** and ***F***). As shown in the examples of Figure 1***F*** and Table 1, although hypertrophy is present in SHR (increase in septum thickness, posterior wall thickness and LVMI), no signs of pump failure were detected, i.e. there were no significant changes in left ventricular diastolic diameter and endocardial and midwall shortening (Table 1). Similarly, the ergometric test was similar between SHR and control rats, i.e. rats stopped running after 8.37±0.82 *vs.* 8.25±0.88 min, respectively.

Ena treatment of SHR prevented the increase in aldosterone plasma levels, indicating the inhibition of RAAS, and slightly but significantly decreased blood pressure (Figure 1***A*** and ***B***). Moreover, the increase in hypertrophic parameters (HW/TL, CSA and LVMI) was also prevented by ACE inhibition (Figure 1***C***-***G*** and table 1).

Figure 2***A*** and ***B*** shows typical blots and average results of P-CaMKII and total CaMKIIδ, and one of its typical substrates, P-Thr^{17} of phospholamban (PLN), and total PLN. There was a significant increment in CaMKII and Thr^{17} phosphorylation in SHR, indicative of CaMKII activation, that was prevented by Ena treatment.

Typical blots and average data of the pro-apoptotic and antiapoptotic proteins Bax and Bcl-2 respectively, the 17-kDa cleavage product of Caspase-3 and TUNEL staining (Figure 3***A,*** and ***B*** respectively) indicated a significantly higher degree of apoptosis in SHR than in age-matched controls, that was prevented by ACE inhibition.

The increase in RAAS produced by Iso treatment induces apoptosis and CaMKII activation in rat hearts

We also investigated whether CaMKII was implicated in inducing apoptosis in another high RAAS activity model produced after 1 month of Iso treatment (4, 16, 30).

As in the case of SHR, high doses of Iso induced an increase in aldosterone plasma levels, blood pressure, and hypertrophy (increased HW/TL relationship and LVMI) (Figure 4***A*** and ***B***) without significant signs of heart failure in the echocargraphic recordings (endocardial and midwall ventricular shortening remains unaltered, Table 2). Moreover, the ergometric test was not different between Iso-rats and their controls (8.50±0.93 *vs* 8.37±0.82 min respectively). Treatment of the animals with Ena significantly decreased the aldosterone plasma levels indicating blockade of the RAAS. Although blood pressure tended to decrease in the Ena treated group, this decrease did not reach significance.

In turn, hypertrophy present in the Iso-rats was prevented by ACE inhibition (Figure 4 ***A*** and ***B*** and Table 2). Consistent with the results obtained in SHR, figure 4***C*** and ***D*** shows that apoptosis (increased TUNEL positive cells, Bax/Bcl-2 ratio and Caspase-3 activation) and the increased CaMKII activity induced by Iso treatment (CaMKII and Thr^{17} site of PLN phosphorylations), were prevented by ACE inhibition with Ena.

Taken together, these results indicate that the enhancement of RAAS in SHR and Iso-rats is associated with a significant increase in CaMKII activity and apoptosis, suggesting a possible causal link between both events *in vivo*. It is worth noting that despite the structural remodeling and apoptosis observed, heart function remains preserved in these rats

CaMKII activity in high RAAS activity models is associated with ROS production and not with Ca^{2+}_i increases

CaMKII activation is conventionally associated with Ca^{2+}_i increments. Moreover recent experiments have emphasized the importance of ROS in the activation of the kinase (see for review, Erikson *et al*., 2011 (10)). We therefore explored Ca^{2+}_i handling and ROS production in an attempt to elucidate the source of CaMKII activation in our models.

We first assessed Ca^{2+}_i handling in isolated myoytes from both high RAAS activity models. Figure 5***A*** shows typical superimposed records of cellular shortening and Ca^{2+}_i transients (CaiT) of the SHR (red traces) and their normotensive controls (black traces). The average results (Figure 5***B***) show that no differences were detected between both groups in contraction amplitude,

CaiT and sarcoplasmic reticulum (SR) Ca^{2+} content, assessed by the amplitude of the caffeine-induced CaiT. Moreover, diastolic and systolic Ca^{2+} did not reach significant difference between SHR and their controls. Mean values were 1.124±0.035 and 1.571±0.059 for control *vs* 1.053±0.031 and 1.556±0.060 for SHR, for diastolic and systolic Fura 2-AM fluorescence, respectively. Similar results were obtained when Iso-rats were compared with their controls. As shown in Figure 5**C**, there were no differences between Iso and control rats in the contraction amplitude, CaiT amplitude or in the SR Ca^{2+} content, suggesting that global Ca^{2+} levels underlying each contractile cycle do not differ between the two groups. These results are in agreement with the absence of signs of cardiac dysfunction (Table 1 and 2 and the ergometric test). The absence of difference in Ca^{2+} handling confirms in *in vivo* models our previous *in vitro* and ex vivo findings, where CaMKII was activated by AngII in the absence of detectable increases in Ca^{2+}_i (28).

In a second set of experiments we estimated oxidative stress by measuring $\cdot O_2^-$ production and lipid peroxidation in SHR, Iso-rats and their controls. Figure 6***A*** shows the increment in $\cdot O_2^-$ generation measured by using lucigenin chemiluminescence in SHR and Iso-rats with respect to control rats. Accordingly, TBARS, used to determine lipid peroxidation, also increased in SHR and Iso-rats compared to their controls (Figure 6***B***). Taken together, these results indicated that the increase in CaMKII in these two models of exacerbated RAAS can not be associated with an enhanced Ca^{2+}_i and occurs together with an increase in ROS production.

Targeted cardiac inhibition of CaMKII prevents apoptosis but does not inhibit ROS production in Iso treated mice

To verify a possible causal link between ROS production, CaMKII activation and apoptosis, we used mice with cardiomyocyte-delimited transgenic expression of either a CaMKII inhibitory peptide (AC3-I) or a scrambled control peptide (AC3-C), after 1 month of Iso treatment. As shown in Figure 7, Iso treatment increased TBARS, an index of lipid peroxidation, in both, AC3-C and AC3-I mice (***A***), indicating an increase in oxidative stress. However, CaMKII activity, measured by the increase in P-CaMKII and in the phosphorylation of Thr^{17} site of PLN (***B***), and apoptosis, assessed by the increase in TUNEL staining (***C***) and the ratio Bax/Bcl2 (***D***), only increased in AC3-C mice. Similarly, Caspase-3 activation was increased in AC3-C mice treated with Iso by 279±73.5 % above control, whereas it did not change significantly in Iso treated AC3-I mice.

These latter results indicate that the increase in ROS that occurred after Iso treatment is upstream of CaMKII activation and that the kinase activity is directly related to the induction of apoptosis.

DISCUSSION

AngII has been shown to be implicated in many cellular physiological and pathological processes. In the long term, the hormone has been associated with cardiomyocyte apoptosis (27, 33, 40). Moreover, experimental evidence indicates that a critical factor in the transition from compensated to non-compensated cardiac hypertrophy is myocyte cell loss by apoptosis (1) and that the circulating levels of AngII are increased in heart failure. It has therefore been proposed that increased AngII levels may constitute one of the major triggers for cell death in the transition to heart failure (20). Interestingly, the onset of AngII plasma or tissue increment during the development of cardiac diseases may start well ahead of the detection of cardiac damage. Moreover, tissue concentrations of AngII are difficult to establish, and they may reach very high levels (over 100 times plasma concentrations) (7) during cardiac remodeling. Thus, to establish the phatophysiological relevance of AngII using *in vitro* experimental tools or animals models where AngII is exogenously administrated, is not straightforward and requires *in vivo* validation. To the best of our knowledge, the *in vivo* effects of enhanced RAAS at an early stage during the development of heart disease have not been previously studied.

In the present study we used two different models of heart disease with exacerbated RAAS well before the appearance of signs or symptoms of heart failure. The main conclusions of our results are the following: 1. Exacerbation of RAAS in these models is an early event necessary to activate CaMKII and to induce cardiac apoptosis; 2. CaMKII activation and cardiomyocyte loss are early signs in the maladaptive processes implicated in the transition from

364 compensated to decompensated left ventricular hypertrophy (13, 22); 3.
365 Activation of CaMKII occurs *in vivo* without detectable Ca^{2+}_i increments and is
366 directly related to the increase in ROS and the induction of apoptosis. These
367 results support the contention that AngII–induced oxidative stress resets the
368 Ca^{2+} dependence of CaMKII, as observed in our previous *in vitro* and *ex vivo*
369 experiments(28).
370
371 *Animals models*
372 The models used are widely known as cardiac hypertrophy and failure models.
373 The SHR model is paradigmatic, since it mimics human essential hypertension
374 and several reports described that endocrine and paracrine RAAS are active
375 (38, 45). Although a variety of factors modify aldosterone secretion, AngII and
376 potassium (43) are the most important regulators. Thus, the increased
377 aldosterone plasma levels found in our animals can be taken as an index of
378 AngII levels, as previously described (2, 45).
379 The Iso-induced cardiac injury model is recognized as one of the toxic
380 cardiomyopathy models of hypertrophy and heart failure (9, 16, 34). Excessive
381 doses of catecholamines produce diffuse myocardial destruction with myocyte
382 loss and necrosis as well as extensive fibrosis in animals and in patients. This
383 kind of damage may be also seen in patients with pheochromocytoma (37). In
384 this model, an exacerbation of RAAS was previously described (16) and
385 confirmed by the present results.
386 In the present work we used these two models of enhanced RAAS at an early
387 stage of disease, as evident by the significant degree of hypertrophy without
388 heart failure signs.

The early signs of heart disease

Typically, heart failure is the culmination of long-standing diseases such as hypertension, ischemia from atherosclerosis, viral myocarditis, valvular insufficiency, or mutations in genes encoding sarcomeric proteins (2, 25). Besides contractile disturbances of cardiomyocytes and interstitial and perivascular fibrosis, cardiomyocyte loss is now being considered as one of the determinant factors of the maladaptive events that negatively impacts the myocardium and its propensity towards failure (12). Although the apoptotic rate observed in the present results is low, rodent studies have implicated low rates of cardiac myocyte apoptosis in the pathogenesis of heart failure. For instance, it has been previously shown that an apoptotic rate as low as 0.023% is sufficient to cause a lethal, dilated cardiomyopathy within 8 to 24 weeks in transgenic mice with cardiac-restricted expression of an inducible caspase-8 allele (41). There is no information concerning the magnitude of cell loss required to depress cardiac contractility in the hypertrophied human heart when cell death occurs (15). Indeed, the apoptotic process takes at most 24 h to be completed and heart failure is a condition that only manifests itself after many years. Thus, it is conceivable that chronic loss of small number of cardiomyocytes on a daily basis can have dramatic consequences on myocardial integrity (36). Moreover, myocardial apoptosis is evident in the myocardium before the occurrence of ventricular dilation and the development of symptoms, which suggests that apoptotis as a causative mechanism rather than a consequence of failure (14). The present results reveal that the increase in apoptotic death as well as the enhanced activity of CaMKII are early events in

these and probably other models with exacerbated RAAS. Since apoptosis paralleled hypertrophy in these two models, the results may indicate that apoptosis represents either an early step in the evolution to heart failure being involved in cardiac remodeling or a mechanism tending to compensate the development of hypertrophy. Further studies are currently in course to discriminate between these possibilities.

Ca^{2+} vs ROS and the role of CaMKII in cardiac disease

CaMKII is typically activated by increments in Ca^{2+}_i and calmodulin (Ca^{2+}/Cam). The complex Ca^{2+}/Cam promotes a conformational change that relieves the autoinhibitory effect of the regulatory domain on the kinase, activating the enzyme. In the sustained presence of Ca^{2+}/Cam, CaMKII undergoes intersubunit autophosphorylation, resulting in Ca^{2+}/Cam independent activity. Recent experimental evidence indicated that ROS-induced oxidation of methionine residues is able to sustain CaMKII activity in the absence of Ca^{2+}/CaM. This action requires however, previous binding of Ca^{2+}/Cam to expose the autoinhibitory domain of CaMKII for oxidation (11). Interestingly, in a previous study we concluded that ROS resets the dependence of CaMKII to Ca^{2+} to extremely low Ca^{2+}_i levels (28). The present results obtained in two different *in vivo* models, are consistent with these previous findings, since the increased activity of CaMKII occurred in the absence of any detectable increase in Ca^{2+}_i but in the presence of a significant increase in ROS production. Our results in transgenic mice further indicate that ROS production is upstream of CaMKII activation in the cascade of events that produces apoptosis after Iso treatment. In this context it is worthwhile to mention that ROS-induced

phosphatase inhibition could also contribute to sustained CaMKII activation *in vivo* (19).

Perspectives

The present results clearly indicate that activation of CaMKII and the associated apoptosis are very early events in the development of heart disease, that are evident even when the only manifestation of the injury is the presence of hypertrophy without any sing or symptom of cardiac dysfunction. They further show that CaMKII activity and apoptosis can both be prevented by inhibition of RAAS. Whether the data can be extrapolated to humans remains to be shown. However, the apoptotic rate obtained in the present results is much lower than the one measured in cardiac tissue from patients with end-stage heart failure, suggesting that apoptosis may also be a causal mechanism of human heart failure. If so, cardiac myocyte apoptosis and CaMKII may constitute novel targets for therapies directed against heart failure. Moreover, in the context of hypertrophy and hypertension, activation of CaMKII could be considered an early index of bad prognosis.

ACKNOWLEDGMENTS

The excellent technical assistance of Andrés Pinilla in echocardiographic imaging is gratefully acknowledged. The assistance of Karina Porzio and Laura Suarez for RIA determinations is also acknowledged.

SOURCES OF FUNDING

This work was supported by Fogarty Grant R03 TW07713 (NIH), PICT 26117 from Agencia Nacional de Promoción Científica y Tecnológica and PIP 2139 from CONICET to AM; and PICT 1041 from Agencia Nacional de Promoción Científica y Tecnológica to JP.

CONFLICT(S) OF INTEREST/DISCLOSURE(S)

None.

REFERENCES

1. **Adams JW, Pagel AL, Means CK, Oksenberg D, Armstrong RC, and Brown JH**. Cardiomyocyte apoptosis induced by Galphaq signaling is mediated by permeability transition pore formation and activation of the mitochondrial death pathway. *Circ Res* 87: 1180-1187, 2000.

2. **Adams KF, Jr.** New epidemiologic perspectives concerning mild-to-moderate heart failure. *Am J Med* 110 Suppl 7A: 6S-13S, 2001.

3. **Beznak M**. Hemodynamics during the acute phase of myocardial damage caused by isoproterenol. *Can J Biochem Physiol* 40: 25-30, 1962.

4. **Beznak M, and Hacker P**. Hemodynamics During the Chronic Stage of Myocardial Damage Caused by Isoproterenol. *Can J Physiol Pharmacol* 42: 269-274, 1964.

5. **Buege JA, and Aust SD**. Microsomal lipid peroxidation. *Methods Enzymol* 52: 302-310, 1978.

6. **Cook SA, Sugden PH, and Clerk A**. Regulation of bcl-2 family proteins during development and in response to oxidative stress in cardiac myocytes: association with changes in mitochondrial membrane potential. *Circ Res* 85: 940-949, 1999.

7. **Dell'Italia LJ, Meng QC, Balcells E, Wei CC, Palmer R, Hageman GR, Durand J, Hankes GH, and Oparil S**. Compartmentalization of angiotensin II generation in the dog heart. Evidence for independent mechanisms in intravascular and interstitial spaces. *J Clin Invest* 100: 253-258, 1997.

8. **Dikalov S, Griendling KK, and Harrison DG**. Measurement of reactive oxygen species in cardiovascular studies. *Hypertension* 49: 717-727, 2007.

9. **El-Demerdash E, Awad AS, Taha RM, El-Hady AM, and Sayed-Ahmed MM**. Probucol attenuates oxidative stress and energy decline in isoproterenol-induced heart failure in rat. *Pharmacol Res* 51: 311-318, 2005.

10. **Erickson JR, He BJ, Grumbach IM, and Anderson ME**. CaMKII in the Cardiovascular System: Sensing Redox States. *Physiol Rev* 91: 889-915.

11. **Erickson JR, Joiner ML, Guan X, Kutschke W, Yang J, Oddis CV, Bartlett RK, Lowe JS, O'Donnell SE, Aykin-Burns N, Zimmerman MC, Zimmerman K, Ham AJ, Weiss RM, Spitz DR, Shea MA, Colbran RJ, Mohler PJ, and Anderson ME**. A dynamic pathway for calcium-independent activation of CaMKII by methionine oxidation. *Cell* 133: 462-474, 2008.

12. **Foo RS, Mani K, and Kitsis RN**. Death begets failure in the heart. *J Clin Invest* 115: 565-571, 2005.

13. **Frohlich ED**. State of the Art lecture. Risk mechanisms in hypertensive heart disease. *Hypertension* 34: 782-789, 1999.

14. **Galiuto L, Lotrionte M, Crea F, Anselmi A, Biondi-Zoccai GG, De Giorgio F, Baldi A, Baldi F, Possati G, Gaudino M, Vetrovec GW, and Abbate A**. Impaired coronary and myocardial flow in severe aortic stenosis is associated with increased apoptosis: a transthoracic Doppler and myocardial contrast echocardiography study. *Heart (British Cardiac Society)* 92: 208-212, 2006.

15. **Gonzalez A, Fortuno MA, Querejeta R, Ravassa S, Lopez B, Lopez N, and Diez J**. Cardiomyocyte apoptosis in hypertensive cardiomyopathy. *Cardiovasc Res* 59: 549-562, 2003.

16. **Grimm D, Elsner D, Schunkert H, Pfeifer M, Griese D, Bruckschlegel G, Muders F, Riegger GA, and Kromer EP**. Development of heart failure

following isoproterenol administration in the rat: role of the renin-angiotensin system. *Cardiovasc Res* 37: 91-100, 1998.

17. **Hagemann D, Bohlender J, Hoch B, Krause EG, and Karczewski P**. Expression of Ca2+/calmodulin-dependent protein kinase II delta-subunit isoforms in rats with hypertensive cardiac hypertrophy. *Mol Cell Biochem* 220: 69-76, 2001.

18. **Hare JM**. Oxidative stress and apoptosis in heart failure progression. *Circ Res* 89: 198-200, 2001.

19. **Howe CJ, Lahair MM, McCubrey JA, and Franklin RA**. Redox regulation of the calcium/calmodulin-dependent protein kinases. *J Biol Chem* 279: 44573-44581, 2004.

20. **Kajstura J, Cigola E, Malhotra A, Li P, Cheng W, Meggs LG, and Anversa P**. Angiotensin II induces apoptosis of adult ventricular myocytes in vitro. *J Mol Cell Cardiol* 29: 859-870, 1997.

21. **Kramer RE, Robinson TV, Schneider EG, and Smith TG**. Direct modulation of basal and angiotensin II-stimulated aldosterone secretion by hydrogen ions. *J Endocrinol* 166: 183-194, 2000.

22. **Levy D, Garrison RJ, Savage DD, Kannel WB, and Castelli WP**. Prognostic implications of echocardiographically determined left ventricular mass in the Framingham Heart Study. *N Engl J Med* 322: 1561-1566, 1990.

23. **Ling YH, Liebes L, Ng B, Buckley M, Elliott PJ, Adams J, Jiang JD, Muggia FM, and Perez-Soler R**. PS-341, a novel proteasome inhibitor, induces Bcl-2 phosphorylation and cleavage in association with G2-M phase arrest and apoptosis. *Mol Cancer Ther* 1: 841-849, 2002.

24. **Litwin SE, Katz SE, Weinberg EO, Lorell BH, Aurigemma GP, and Douglas PS**. Serial echocardiographic-Doppler assessment of left ventricular geometry and function in rats with pressure-overload hypertrophy. Chronic angiotensin-converting enzyme inhibition attenuates the transition to heart failure. *Circulation* 91: 2642-2654, 1995.

25. **Lloyd-Jones DM, Larson MG, Leip EP, Beiser A, D'Agostino RB, Kannel WB, Murabito JM, Vasan RS, Benjamin EJ, and Levy D**. Lifetime risk for developing congestive heart failure: the Framingham Heart Study. *Circulation* 106: 3068-3072, 2002.

26. **Mundina-Weilenmann C, Vittone L, Ortale M, de Cingolani GC, and Mattiazzi A**. Immunodetection of phosphorylation sites gives new insights into the mechanisms underlying phospholamban phosphorylation in the intact heart. *J Biol Chem* 271: 33561-33567, 1996.

27. **Palomeque J, Delbridge L, and Petroff MV**. Angiotensin II: a regulator of cardiomyocyte function and survival. *Front Biosci* 14: 5118-5133, 2009.

28. **Palomeque J, Rueda OV, Sapia L, Valverde CA, Salas M, Petroff MV, and Mattiazzi A**. Angiotensin II-induced oxidative stress resets the Ca2+ dependence of Ca2+-calmodulin protein kinase II and promotes a death pathway conserved across different species. *Circ Res* 105: 1204-1212, 2009.

29. **Palomeque J, Sapia L, Hajjar RJ, Mattiazzi A, and Vila Petroff M**. Angiotensin II-induced negative inotropy in rat ventricular myocytes: role of reactive oxygen species and p38 MAPK. *Am J Physiol Heart Circ Physiol* 290: H96-106, 2006.

570 30. **Rona G, Chappel CI, Balazs T, and Gaudry R**. An infarct-like
571 myocardial lesion and other toxic manifestations produced by isoproterenol in
572 the rat. *AMA Arch Pathol* 67: 443-455, 1959.
573 31. **Sahn DJ, DeMaria A, Kisslo J, and Weyman A**. Recommendations
574 regarding quantitation in M-mode echocardiography: results of a survey of
575 echocardiographic measurements. *Circulation* 58: 1072-1083, 1978.
576 32. **Salas MA, Valverde CA, Sanchez G, Said M, Rodriguez JS,**
577 **Portiansky EL, Kaetzel MA, Dedman JR, Donoso P, Kranias EG, and**
578 **Mattiazzi A**. The signalling pathway of CaMKII-mediated apoptosis and
579 necrosis in the ischemia/reperfusion injury. *J Mol Cell Cardiol* 48: 1298-1306,
580 2010.
581 33. **Sorescu D, and Griendling KK**. Reactive oxygen species, mitochondria,
582 and NAD(P)H oxidases in the development and progression of heart failure.
583 *Congest Heart Fail* 8: 132-140, 2002.
584 34. **Teerlink JR, Pfeffer JM, and Pfeffer MA**. Progressive ventricular
585 remodeling in response to diffuse isoproterenol-induced myocardial necrosis in
586 rats. *Circ Res* 75: 105-113, 1994.
587 35. **Tojo A, Onozato ML, Kobayashi N, Goto A, Matsuoka H, and Fujita**
588 **T**. Angiotensin II and oxidative stress in Dahl Salt-sensitive rat with heart failure.
589 *Hypertension* 40: 834-839, 2002.
590 36. **van Empel VP, Bertrand AT, Hofstra L, Crijns HJ, Doevendans PA,**
591 **and De Windt LJ**. Myocyte apoptosis in heart failure. *Cardiovasc Res* 67: 21-
592 29, 2005.
593 37. **Van Vliet PD, Burchell HB, and Titus JL**. Focal myocarditis associated
594 with pheochromocytoma. *N Engl J Med* 274: 1102-1108, 1966.

595 38. **Varagic J, and Frohlich ED**. Local cardiac renin-angiotensin system:
596 hypertension and cardiac failure. *J Mol Cell Cardiol* 34: 1435-1442, 2002.
597 39. **Vila-Petroff M, Salas MA, Said M, Valverde CA, Sapia L, Portiansky**
598 **E, Hajjar RJ, Kranias EG, Mundina-Weilenmann C, and Mattiazzi A**. CaMKII
599 inhibition protects against necrosis and apoptosis in irreversible ischemia-
600 reperfusion injury. *Cardiovasc Res* 73: 689-698, 2007.
601 40. **Vivar R, Soto C, Copaja M, Mateluna F, Aranguiz P, Munoz JP,**
602 **Chiong M, Garcia L, Letelier A, Thomas WG, Lavandero S, and Diaz-Araya**
603 **G**. Phospholipase C/protein kinase C pathway mediates angiotensin II-
604 dependent apoptosis in neonatal rat cardiac fibroblasts expressing AT1
605 receptor. *J Cardiovasc Pharmacol* 52: 184-190, 2008.
606 41. **Wencker D, Chandra M, Nguyen K, Miao W, Garantziotis S, Factor**
607 **SM, Shirani J, Armstrong RC, and Kitsis RN**. A mechanistic role for cardiac
608 myocyte apoptosis in heart failure. *J Clin Invest* 111: 1497-1504, 2003.
609 42. **Whelan RS, Kaplinskiy V, and Kitsis RN**. Cell death in the
610 pathogenesis of heart disease: mechanisms and significance. *Annu Rev Physiol*
611 72: 19-44, 2010.
612 43. **Williams GH**. Aldosterone biosynthesis, regulation, and classical
613 mechanism of action. *Heart Fail Rev* 10: 7-13, 2005.
614 44. **Yamamoto K, Ichijo H, and Korsmeyer SJ**. BCL-2 is phosphorylated
615 and inactivated by an ASK1/Jun N-terminal protein kinase pathway normally
616 activated at G(2)/M. *Mol Cell Biol* 19: 8469-8478, 1999.
617 45. **Yoneda M, Sanada H, Yatabe J, Midorikawa S, Hashimoto S, Sasaki**
618 **M, Katoh T, Watanabe T, Andrews PM, Jose PA, and Felder RA**. Differential

effects of angiotensin II type-1 receptor antisense oligonucleotides on renal function in spontaneously hypertensive rats. *Hypertension* 46: 58-65, 2005.

46. **Zhang T, and Brown JH**. Role of Ca2+/calmodulin-dependent protein kinase II in cardiac hypertrophy and heart failure. *Cardiovas Res* 63: 476-486, 2004.

47. **Zhu W, Woo AY, Yang D, Cheng H, Crow MT, and Xiao RP**. Activation of CaMKIIdeltaC is a common intermediate of diverse death stimuli-induced heart muscle cell apoptosis. *J Biol Chem* 282: 10833-10839, 2007.

LEGENDS TO THE FIGURES

Figure 1. ***High RAAS activity induced-hypertrophy in SHR is reversed by angiotensin converting enzyme (ACE) inhibition***. Aldostrone plasma levels, expressed as percentage of control values (***A***), systolic blood pressure values (***B***) and hypertrophic parameters (***C*** to ***G***). ***C***, heart weight/tibia length (HW/TL) ratio; ***D*** and ***E***; cross sectional area (CSA) of the myocytes; and ***F*** and ***G***; left ventricular mass, ***F***, representative echocardiographic images and ***G***, normalized by tibia length (LVMI); are significantly increased in SHR. Enalapril (Ena) treatment prevents the increments in all the parameters studied (***A***-***G***). Here and in Figure 4, Sp Th, means septum thickness; Dd, diastolic diameter; Pw Th, posterior wall thickness. In this and the following figures overall data are expressed as means ± S.E.M. * $p<0.05$, *vs*. control. § $p<0.05$ +Ena *vs* SHR. The n of each experimental group is presented between brackets in the figures.

Figure 2. ***Enalapril (Ena) blunts CaMKII activity in SHR. A***, typical blots of the phosphorylated form of CaMKII (P-CaMKII) and of its substrate, phospho-Thr^{17} residue of phospholamban (P-Thr^{17}) in control rats, SHR and SHR treated with Ena. Total CaMKIIδ and PLN expression are also shown. SHR depicted an increment in both phospho proteins and the treatment with Ena prevented both phosphorylations. ***B***, average data of these experiments. The signals of P-CaMKII and P-Thr^{17} were normalized by their total respective proteins. These experiments revealed that CaMKII is being activated by Ang II.

Figura 3. ***Cardiac apoptosis in SHR is prevented by Enalapril (Ena). A***, representative blots and average data of the pro-apoptotic and antiapoptotic proteins Bax and Bcl-2, respectively and the 17-kDa cleavage product of Caspase-3 from control rats, SHR and SHR treated with Ena. GAPDH signals were used as loading controls. The increased ratio Bax/Bcl-2, used as an apoptotic index, and Caspase-3 activation in SHR is prevented by Ena treatment. ***B***, typical photographs of TUNEL assay and DAPI staining of control, SHR and SHR treated with Ena. The mean values of TUNEL positive cells normalized by total DAPI stained nuclei in the bar graph below, indicates that the increment in apoptosis in SHR is prevented by blocking RAAS axis.

Figure 4*. Enalapril treatment prevents Iso-induced hypertrophy, CaMKII activation and apoptosis. A*, from left to right, aldosterone plasma levels, blood pressure, and the hypertrophic indexes, heart weight/tibia length (HW/TL) and the left ventricular mass index (LVMI) measured by echocardiography, from control rats, Iso and Iso+Ena treated rats. All the parameters show an increment in Iso-rats which is prevented by the co-treatment with Ena. ***B***, representative echocardiographic images of the groups examined in ***A***. ***C***, TUNEL and DAPI photographs of the different groups and mean values of these experiments indicating an increment in TUNEL positive cells normalized by total DAPI stained nuclei, only in Iso-rats. ***D,*** typical blots and average data of P-CaMKII and its substrate, P-Thr^{17} of PLN; of apoptotic and anti-apoptotic proteins, Bax and Bcl-2, respectively; and of active Caspase-3 from control, Iso and Iso+Ena groups. Total CaMKIIδ, PLN and GAPDH are also shown. Iso treatment induces an increase in CaMKII activity (P-CaMKII and P-Thr^{17}), in the

apoptotic index (Bax/Bcl-2 ratio) and in Caspase-3 activation which are prevented by Ena treatment. These groups of experiments link the increase in RAAS activity with apoptosis and CaMKII activation. ¤ $p<0.05$ +Ena *vs* Iso.

Figure 5. ***Unaltered Ca^{2+} handling in control rats, SHR and Iso-treated rats.*** ***A***, representative superimposed recording of cell length and CaiT from isolated myocytes of control rats (black trace) and SHR (red trace). The contraction amplitude and the CaiT amplitude under field stimulated conditions (0.5Hz) or under caffeine pulse (25 mmol/L) were not different between the strains. Average data of these experiments are depicted in ***B***. ***C*** mean values of these parameters comparing control with Iso-rats. There were no significant differences in any of the variables studied between SHR or Iso-rats with respect to their controls.

Figure 6. $\cdot O_2^-$ and lipid peroxidation are increased in SHR and Iso-rats. ***A***, $\cdot O_2^-$ generation by myocardial slices from control (■), Iso (▲) and SHR (○). Both Iso and SHR display a significant increase in $\cdot O_2^-$ production. The data fitted with a one phase exponential association (GraphPad Prism 4.2) from SHR and Iso-rats were significantly higher than the control curve. For better comparison, the bar graph below depicts the mean values at 20 min, when the reaction was completely stabilized, showing a significant increment in $\cdot O_2^-$ generation in Iso and SHR with respect to control rats. ***B***, average data of TBARS indicating that SHR and Iso rats present higher levels of lipid peroxidation than control rats.

Figure 7. ***Mice with cardiomyocyte-delimited transgenic expression of CaMKII inhibitory peptide are protected from Iso-induced apoptosis. A***, lipid peroxidation measured by TBARS indicates that Iso treatment increases oxidative stress both in AC3-C and AC3-I mice. ***B***, TUNEL and DAPI photographs of the different groups and mean values of these experiments indicating a significant increment in TUNEL positive cells normalized by total DAPI stained nuclei only in the AC3-C mice treated with Iso. ***C***, representative blots from P-CaMKII and P-Thr^{17}, and their respective total proteins, as an index of CaMKII activity, and average results, show that under Iso treatment only AC3-C mice increase phosphorylation of CaMKII and PLN at the CaMKII site. ***D***, typical blots of pro- and anti-apoptotic protein Bax, and Bcl-2, and mean results in the bar graph below. GAPDH signals were used as loading controls. Iso treatment induced apoptosis only in AC3-C mice.

Table 1. Echocardiographic parameters from control rats, SHR and SHR treated with Enalapril.

	Control	SHR	SHR+Enalapril
N	9	8	6
LVDD (mm)	5.59 ± 0.32	6.44 ± 0.16	6.07 ± 0.11
STh (mm)	1.52 ± 0.03 *	1.85 ± 0.03 *	1.71 ± 0.02 *
LVPWTh (mm)	1.55 ± 0.02 *	1.92 ± 0.06 *	1.70 ± 0.03 *
ES (%)	60.76 ± 0.89	60.87 ± 0.46	61.39 ± 1.34
MVS (%)	30.60 ± 1.51	30.53 ± 0.96	30.66 ± 0.77
LVMI (mg/g)	1.39 ± 0.09 *	2.61 ± 0.12 *	2.04 ± 0.05 *
LVMI (mg/mm)	12.79 ± 1.05 *	21.43 ± 1.15 *	17.81 ± 0.39 *

Values are mean ± ES. LVDD: Left ventricular diastolic diameter; STh: septum thickness; LVPWTh: left ventricular posterior wall thickness; ES: endocardial shortening; MVS: midwall ventricular shortening; LVMI: left ventricular mass index. * $p<0.05$ *vs* all others groups.

748 **Table 2.** Echocardiographic parameters from control rats, Iso-rats and Iso-rats
749 treated with Enalapril
750

	Wistar (A)	Wistar Isoproterenol (B)	Wistar+ Enalapril (C)	Wistar Isoproterenol +Enalapril (D)
n	12	29	4	7
LVDD (mm)	5.20 ± 0.13 *	5.81 ± 0.07 *	3.72 ± 0.12 *	4.43 ± 0.23 *
STh (mm)	1.54 ± 0.03 ‡	1.64 ± 0.02 †	1.26 ± 0.02 † ‡	1.23 ± 0.05 † ‡
LVPWTh (mm)	1.56 ± 0.02 ‡	1.70 ± 0.02 †	1.24 ± 0.02 † ‡	1.22 ± 0.04 † ‡
ES (%)	60.76 ± 0.70	59.86 ± 0.40	58.98 ± 1.0	58.52 ± 0.86
MVS (%)	30.16 ± 1.32	33.03 ± 0.90	33.1 ± 1.02	34.52 ± 0.91
LVMI (mg/g)	1.38 ± 0.08	1.91 ± 0.04 †	1.70 ± 0.04 †	1.71 ± 0.04 † ‡
LVMI(mg/mm)	11.18 ± 0.47 ‡	14.28 ± 0.36 †	5.16 ± 0.06 † ‡	6.76 ± 0.91 † ‡

751
752 Values are mean ± ES. LVDD: Left ventricular diastolic diameter; STh: septum
753 thickness; LVPWTh: left ventricular posterior wall thickness; ES: endocardial
754 shortening; MVS: midwall ventricular shortening; LVMI: left ventricular mass
755 index. * p<0.05 *vs* all others groups; † p< 0.05 *vs* A; ‡ p< 0.05 *vs* B.

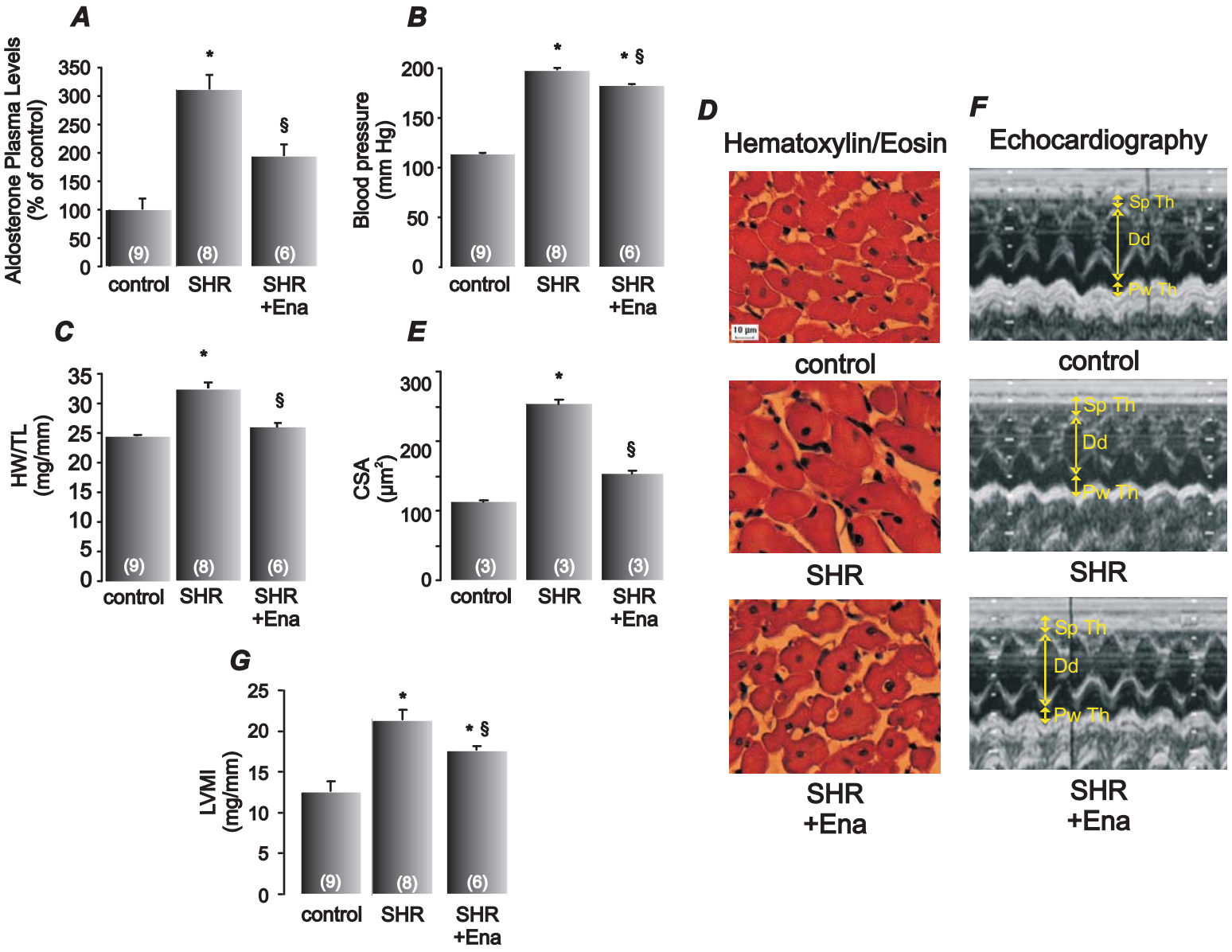
A
Aldosterone Plasma Levels (% of control)
350
300
250
200
150
100
50
0
*
§
(9)
(8)
(6)
control
SHR
SHR +Ena
B
Blood pressure (mm Hg)
200
150
100
50
0
*
* §
(9)
(8)
(6)
control
SHR
SHR +Ena
C
HW/TL (mg/mm)
35
30
25
20
15
10
5
0
*
§
(9)
(8)
(6)
control
SHR
SHR +Ena
E
CSA (µm²)
300
200
100
0
*
§
(3)
(3)
(3)
control
SHR
SHR +Ena
G
LVMI (mg/mm)
25
20
15
10
5
0
*
* §
(9)
(8)
(6)
control
SHR
SHR +Ena
D
Hematoxylin/Eosin
10 µm
control
SHR
SHR +Ena
F
Echocardiography
Sp Th
Dd
Pw Th
control
SHR
SHR +Ena

Figure 1

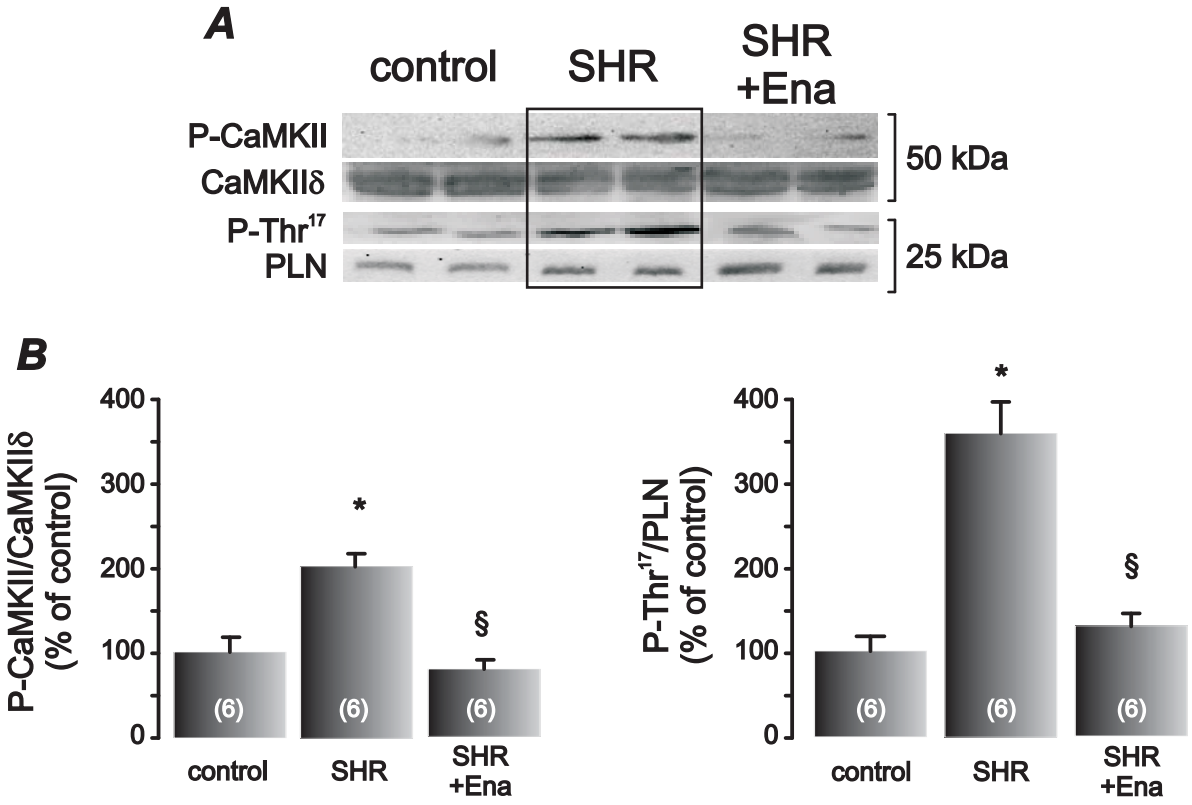
A
control
SHR
SHR +Ena
P-CaMKII
CaMKIIδ
P-Thr17
PLN
50 kDa
25 kDa
B
P-CaMKII/CaMKIIδ (% of control)
400
300
200
100
0
*
§
(6)
(6)
(6)
control
SHR
SHR +Ena
P-Thr17/PLN (% of control)
400
300
200
100
0
*
§
(6)
(6)
(6)
control
SHR
SHR +Ena

Figure 2

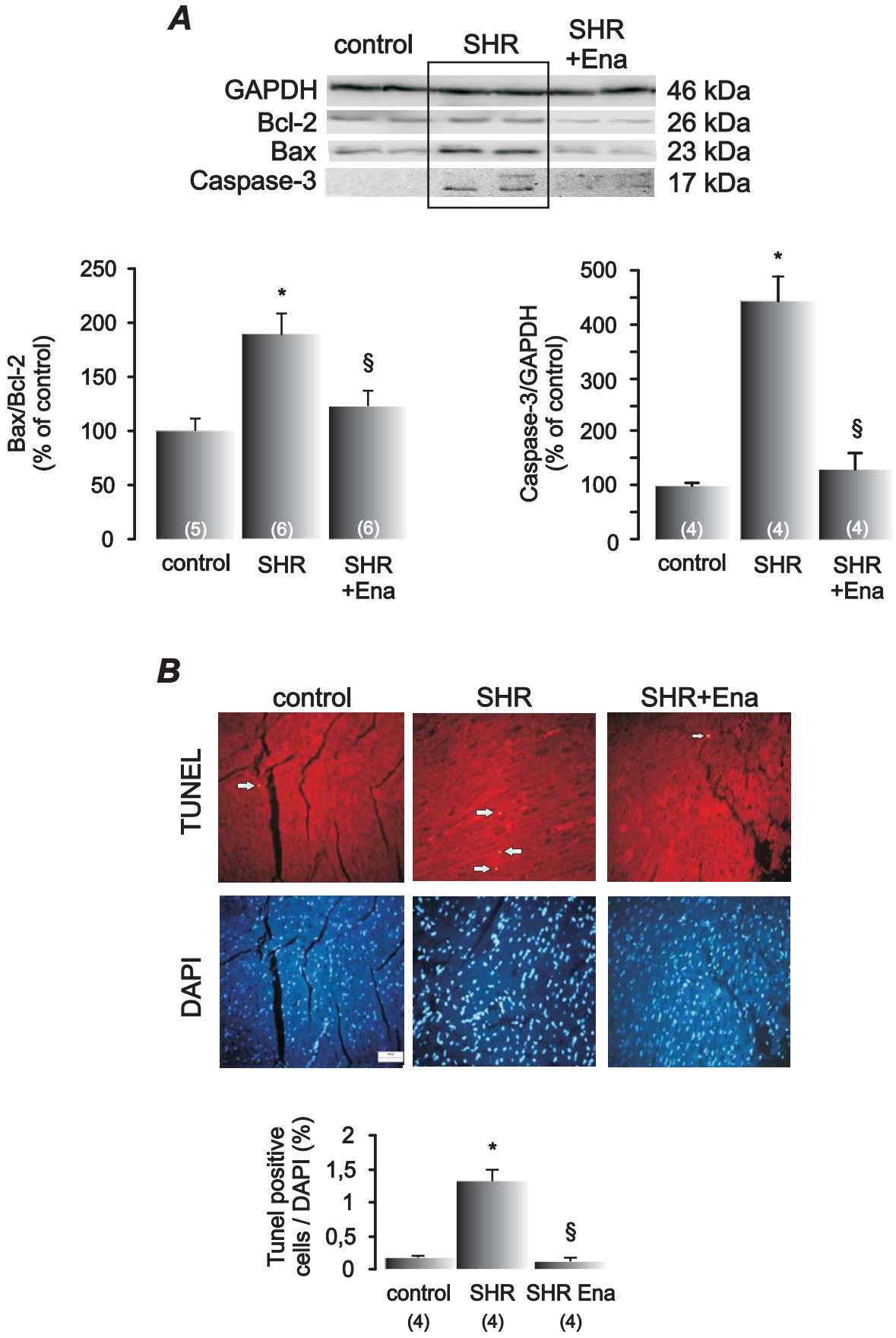
A
control
SHR
SHR +Ena
GAPDH
Bcl-2
Bax
Caspase-3
46 kDa
26 kDa
23 kDa
17 kDa
Bax/Bcl-2 (% of control)
250
200
150
100
50
0
*
§
(5)
(6)
(6)
control
SHR
SHR +Ena
Caspase-3/GAPDH (% of control)
500
400
300
200
100
0
*
§
(4)
(4)
(4)
control
SHR
SHR +Ena
B
control
SHR
SHR+Ena
TUNEL
DAPI
Tunel positive cells / DAPI (%)
2
1,5
1
0,5
0
*
§
control
(4)
SHR
(4)
SHR Ena
(4)

Figure 3

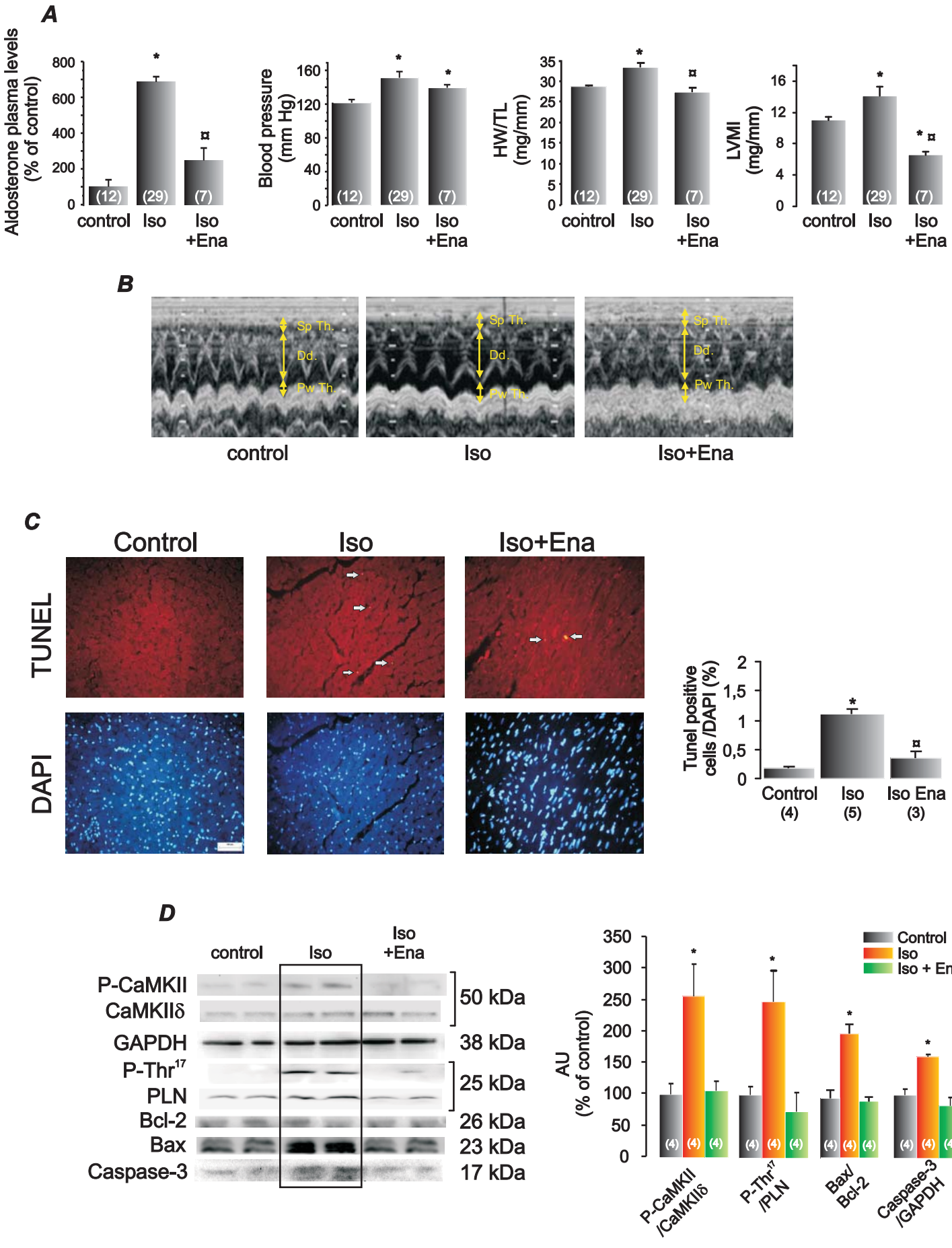
A
Aldosterone plasma levels (% of control)
800
600
400
200
0
(12)
(29)
(7)
control
Iso
Iso +Ena
Blood pressure (mm Hg)
160
120
80
40
0
HW/TL (mg/mm)
35
30
25
20
15
10
5
0
LVMI (mg/mm)
16
12
8
4
0
B
Sp Th.
Dd.
Pw Th.
control
Iso
Iso+Ena
C
Control
Iso
Iso+Ena
TUNEL
DAPI
Tunel positive cells /DAPI (%)
2
1,5
1
0,5
0
Control (4)
Iso (5)
Iso Ena (3)
D
control
Iso
Iso +Ena
P-CaMKII
CaMKIIδ
GAPDH
P-Thr17
PLN
Bcl-2
Bax
Caspase-3
50 kDa
38 kDa
25 kDa
26 kDa
23 kDa
17 kDa
AU (% of control)
350
300
250
200
150
100
50
0
Control
Iso
Iso + Ena
P-CaMKII /CaMKIIδ
P-Thr17 /PLN
Bax/ Bcl-2
Caspase-3 /GAPDH

Figure 4

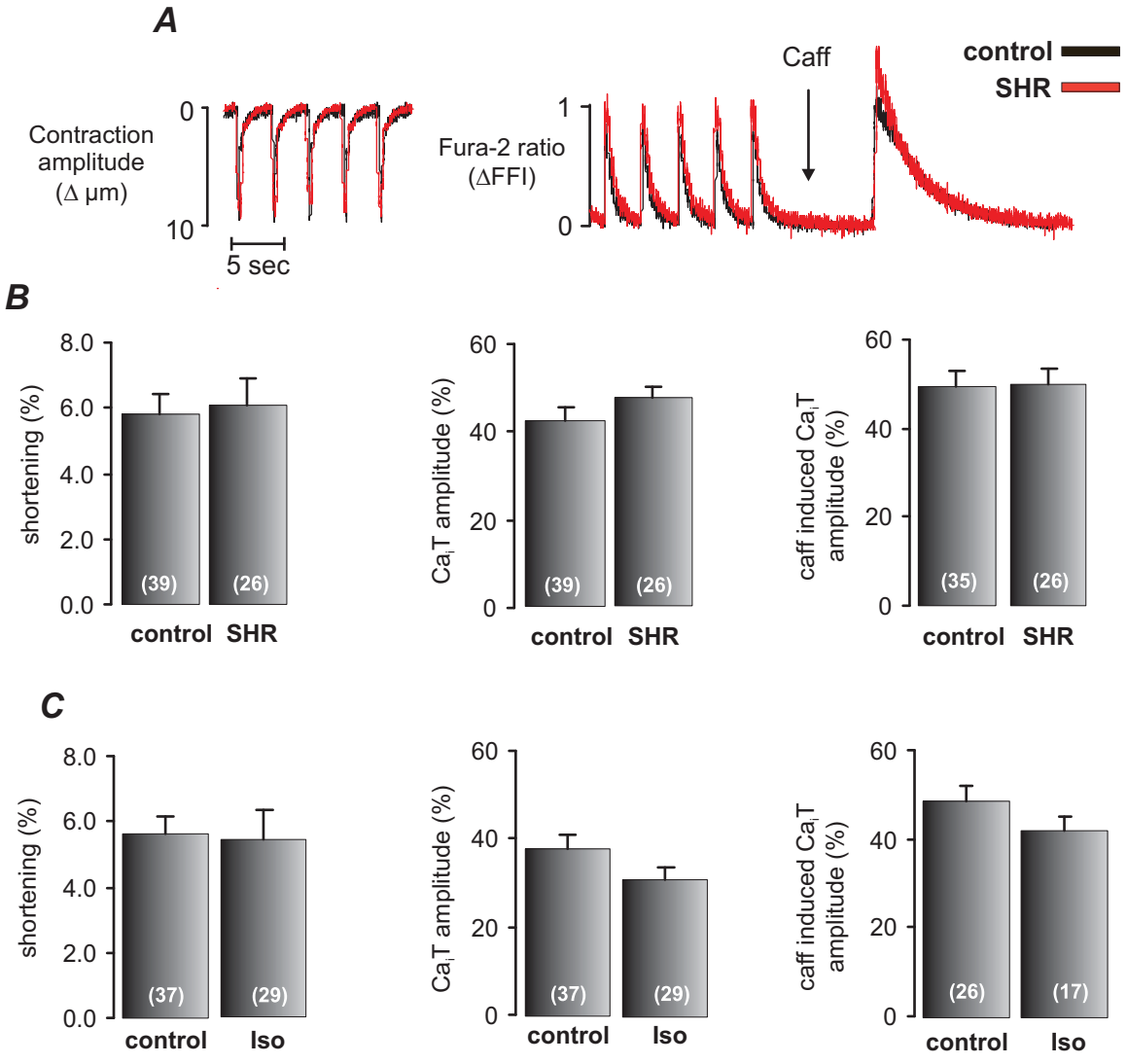
A
Contraction amplitude (Δ µm)
0
10
5 sec
Caff
control
SHR
Fura-2 ratio (ΔFFI)
1
0
B
shortening (%)
8.0
6.0
4.0
2.0
0.0
(39)
(26)
control
SHR
Ca$_i$T amplitude (%)
60
40
20
0
(39)
(26)
control
SHR
caff induced Ca$_i$T amplitude (%)
60
40
20
0
(35)
(26)
control
SHR
C
shortening (%)
8.0
6.0
4.0
2.0
0.0
(37)
(29)
control
Iso
Ca$_i$T amplitude (%)
60
40
20
0
(37)
(29)
control
Iso
caff induced Ca$_i$T amplitude (%)
60
40
20
0
(26)
(17)
control
Iso

Figure 5

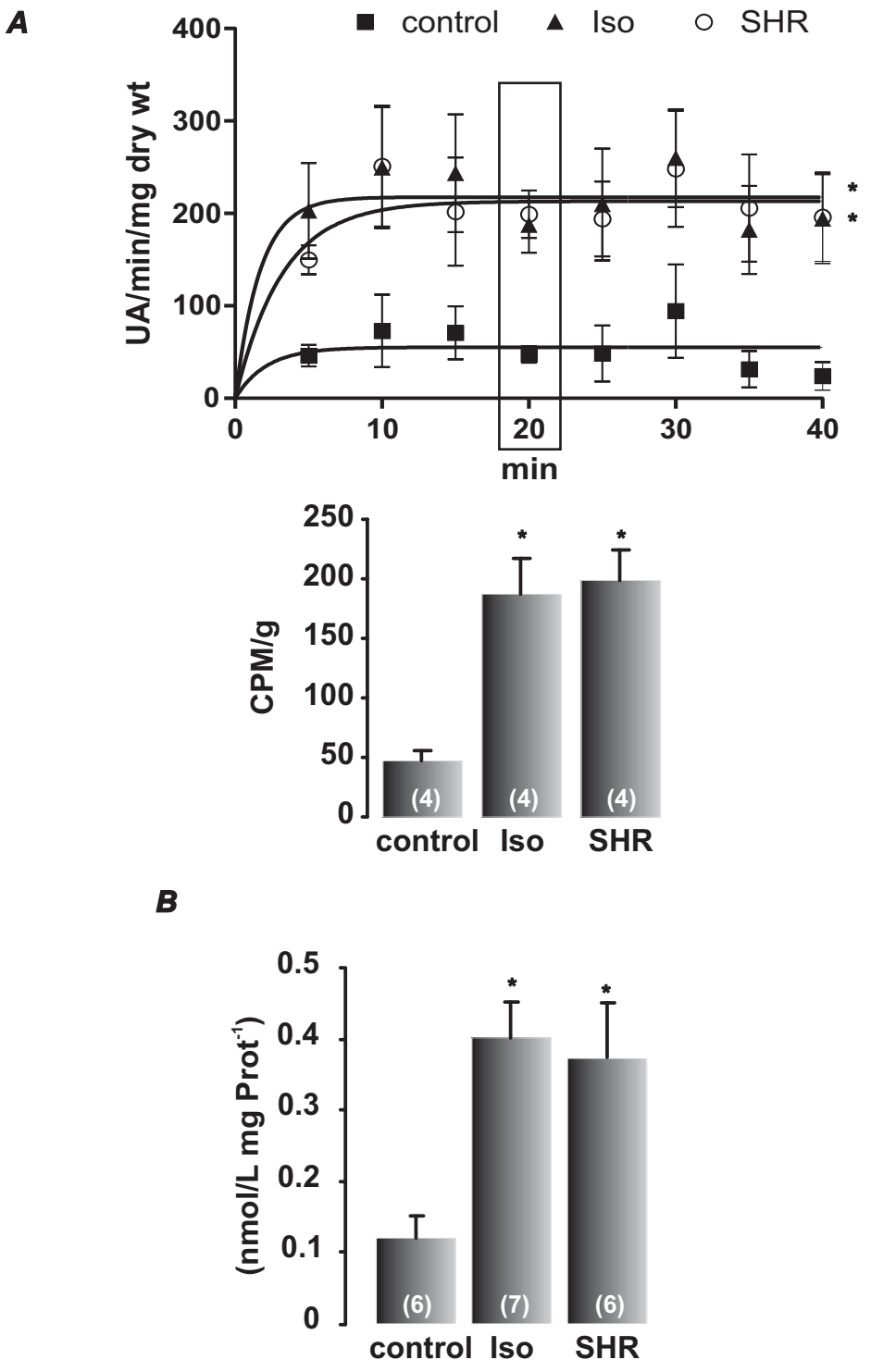
A
control
Iso
SHR
UA/min/mg dry wt
400
300
200
100
0
0
10
20
30
40
min
*
*
CPM/g
250
200
150
100
50
0
*
*
(4)
(4)
(4)
control
Iso
SHR
B
(nmol/L mg Prot-1)
0.5
0.4
0.3
0.2
0.1
0
*
*
(6)
(7)
(6)
control
Iso
SHR

Figure 6

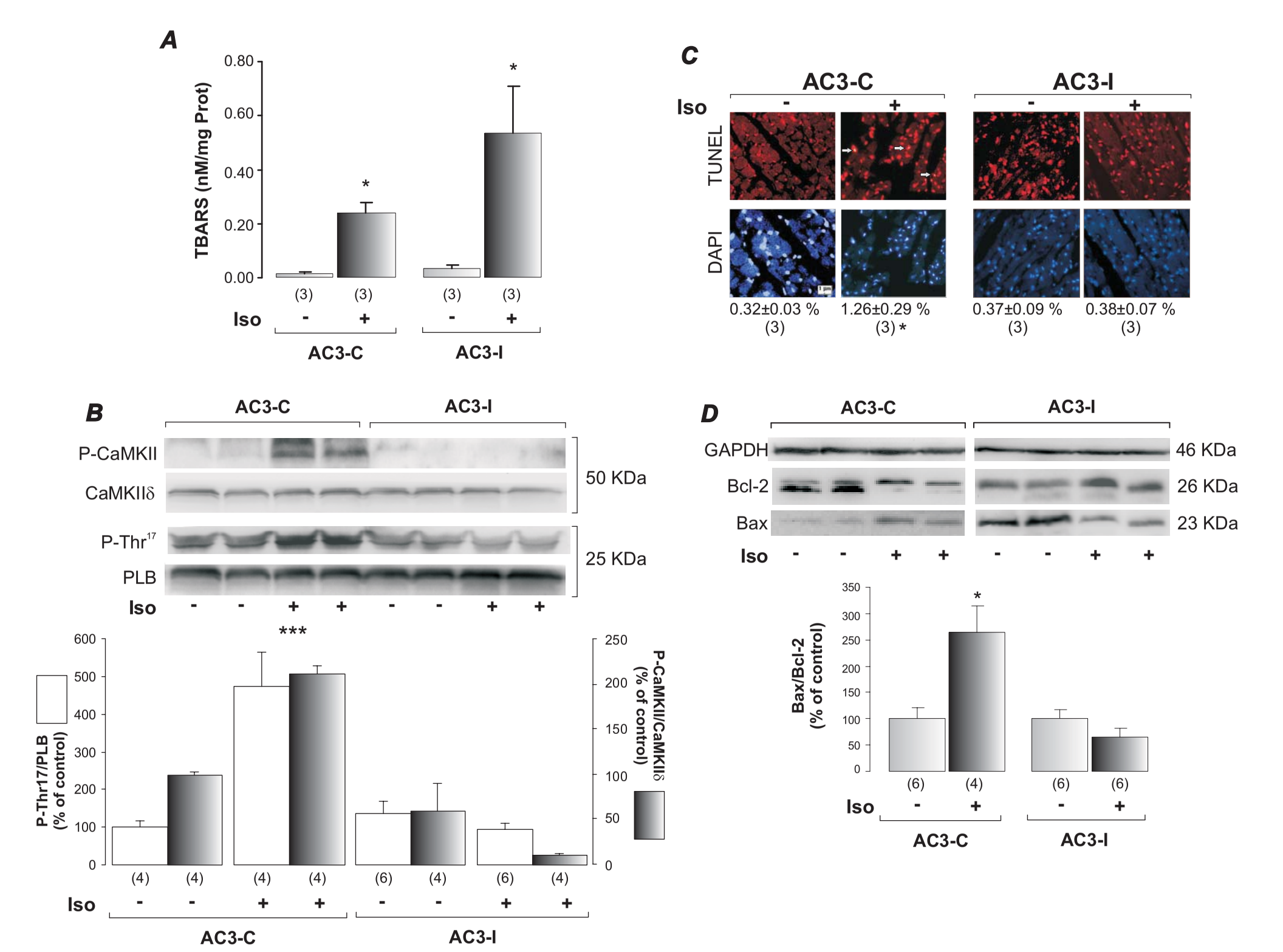
A
TBARS (nM/mg Prot)
0.80
0.60
0.40
0.20
0.00
*
*
(3) (3) (3) (3)
Iso - + - +
AC3-C
AC3-I
C
AC3-C
AC3-I
Iso - + - +
TUNEL
DAPI
0.32±0.03 %
(3)
1.26±0.29 %
(3) *
0.37±0.09 %
(3)
0.38±0.07 %
(3)
B
AC3-C
AC3-I
P-CaMKII
CaMKIIδ
50 KDa
P-Thr17
PLB
25 KDa
Iso - - + + - - + +
***
P-Thr17/PLB (% of control)
P-CaMKII/CaMKIIδ (% of control)
600
500
400
300
200
100
0
250
200
150
100
50
0
(4) (4) (4) (4) (6) (4) (6) (4)
Iso - - + + - - + +
AC3-C
AC3-I
D
AC3-C
AC3-I
GAPDH
Bcl-2
Bax
46 KDa
26 KDa
23 KDa
Iso - - + + - - + +
Bax/Bcl-2 (% of control)
350
300
250
200
150
100
50
0
*
(6) (4) (6) (6)
Iso - + - +
AC3-C
AC3-I

Figure 7